Journal of Chemical Health Risks

www.jchr.org

JCHR (2025) 15(3), 2601-2618 | ISSN:2251-6727

In Silico Characterization and Functional Insights into the Role of GSK-3 Beta in Lung Cancer

Rajesh Kumar[1], Saransh[1], Ketan Chandra[1], Archit Sharma[1*]

Department of Biotechnology, University Institute of Engineering and Technology, Kurukshetra University, Kurukshetra

(Received: 16 March 2025 Revised: 20 April 2025 Accepted: 15 June 2025)

KEYWORDS

GSK-3 Beta, lung cancer, in silico analysis, structural bioinformatics, cancer risk, chemical health, protein modelling

ABSTRACT:

Background: Glycogen Synthase Kinase 3 Beta (GSK-3β) plays a key role in various biochemical pathways, including those involved in cellular metabolism, tumorigenesis, and oxidative stress responses. Given the increasing recognition of environmental and chemical contributors to cancer development, understanding the molecular characteristics of GSK-3β in lung cancer may offer insights into potential chemical health risks and therapeutic interventions.

Materials and Methods: The amino acid sequence and structure of GSK-3β (PDB ID: 1MQB) were analyzed using multiple in silico tools. Primary sequence analysis was conducted with ProtParam, secondary structure prediction using SOPMA, and 3D modelling via SWISS-MODEL. Structural validation was carried out with PROCHECK. Protein–protein interaction networks were explored using STRING.

Results and Conclusion: GSK-3β demonstrated high structural stability and integrity, supporting its crucial involvement in cancer cell metabolism, autophagy regulation, and tumour progression. STRING analysis revealed a dense interaction network, emphasizing GSK-3β's centrality in lung cancer pathways. These findings suggest that GSK-3β could serve as a molecular link between biochemical dysregulation and potential chemical-induced carcinogenesis, warranting further investigation from both therapeutic and health risk perspectives.

Introduction

Cancer is a group of diseases characterized by the development of abnormal cells that divide uncontrollably and can infiltrate and destroy normal body tissue. It is the second leading cause of mortality worldwide and a serious problem affecting the health of all human societies [1]. Cancer can arise from a range of external influences, like tobacco use, exposure to chemicals, radiation, or infectious agents. It can also be triggered by internal factors, such as genetic mutations, hormonal imbalances, immune system disorders, and spontaneous mutations. The origins of cancer are varied, intricate, and only partly comprehended. Many things are known to increase the risk of cancer including dietary factors, certain infections, lack of physical activity, obesity, and environmental pollutants [2].

Lung cancer is the third most common type of cancer in the US and leading cause of cancer-related deaths in Asia. Lung cancer, also known as 'lung carcinoma,' is a cancerous growth that begins in lung tissues. It is characterized by the uncontrolled growth of abnormal lung cells [3]. Genetic mutations and epigenetic alterations are the main factors contributing to the development of lung cancer. Risk factors such as tobacco smoking and exposure to carcinogens can lead to genetic mutations. The disruption of key processes like cell proliferation, differentiation, and apoptosis is a significant factor in the development of this disease. GSK-3 Beta, a major protein, is linked to lung cancer through its dysregulation [4]. Metabolic changes in cancer cells lead to varying metabolite concentration levels in the plasma of lung cancer patients when compared to healthy individuals and those with inflammatory diseases.

GSK-3 Beta is a serine/threonine protein kinase involved in numerous biological and pathological processes, such as regulating energy metabolism, modulating insulin sensitivity, and responding to stress. In the context of lung cancer, GSK-3 Beta has been shown to play diverse roles in different tissues, including serving as a negative regulator of beneficial effects in the liver, skeletal muscle, and pancreas, and as a positive regulator of harmful effects in the heart and white adipose tissue. In lung cancer cells, GSK-3 Beta has been found to regulate myogenesis negatively, inhibit the induction of muscle

Journal of Chemical Health Risks
www.jchr.org
JCHR (2025) 15(3), 2601-2618 | ISSN:2251-6727

atrophy, and enhance skeletal muscle mitochondrial oxidative metabolism [5]. Moreover, physical exercise significantly decreases GSK-3 Beta activity, potentially initiating enhanced muscle protein metabolism and improved muscle function, both of which play a role in regulating energy metabolism.

GSK-3 Beta has been shown to play a critical role in regulating glycogen synthesis and glucose metabolism in the liver, skeletal muscle, and other tissues [6]. However, the impact of GSK-3 Beta on glucose metabolism and insulin function is complex and may vary by tissue type, genetic strain, or even species. In addition to its well-known substrates like GS, GSK-3 Beta may have other unidentified substrates that are crucial in regulating metabolic phenotypes.

In terms of lung cancer, GSK-3 Beta is involved in the regulation of tumour metabolism and growth. In certain types of cancers, such as colon, liver, ovarian, and pancreatic tumours, GSK-3 Beta is overexpressed and promotes tumour growth [7]. In contrast, in other types of cancer, such as renal cancer, prostate cancer, and breast cancer cells GSK-3 Beta has been found to promote cancer cell survival and to regulate autophagy. Further research is needed to fully understand the significance of GSK-3 Beta in lung cancer and to develop potential therapeutic strategies targeting GSK-3 Beta in this context.

In silico protein analysis is highly significant for utilizing data in drug development and healthcare advancements. During the initial stages of drug development, computational methods are valuable for predicting toxicity, refining processes, and uncovering promising compounds, leading to efficiency gains and cost savings. Despite their significance, these in-silico techniques cannot fully substitute the essential in vitro and in vivo testing procedures. This technique aids in the discovery of new markers and treatment objectives for lung cancer. The in-silico experimentation involves utilizing computer models to simulate biological systems and make predictions based on biological data, enabling investigations conducted solely through computer-based methods [8].

Material and Methodology

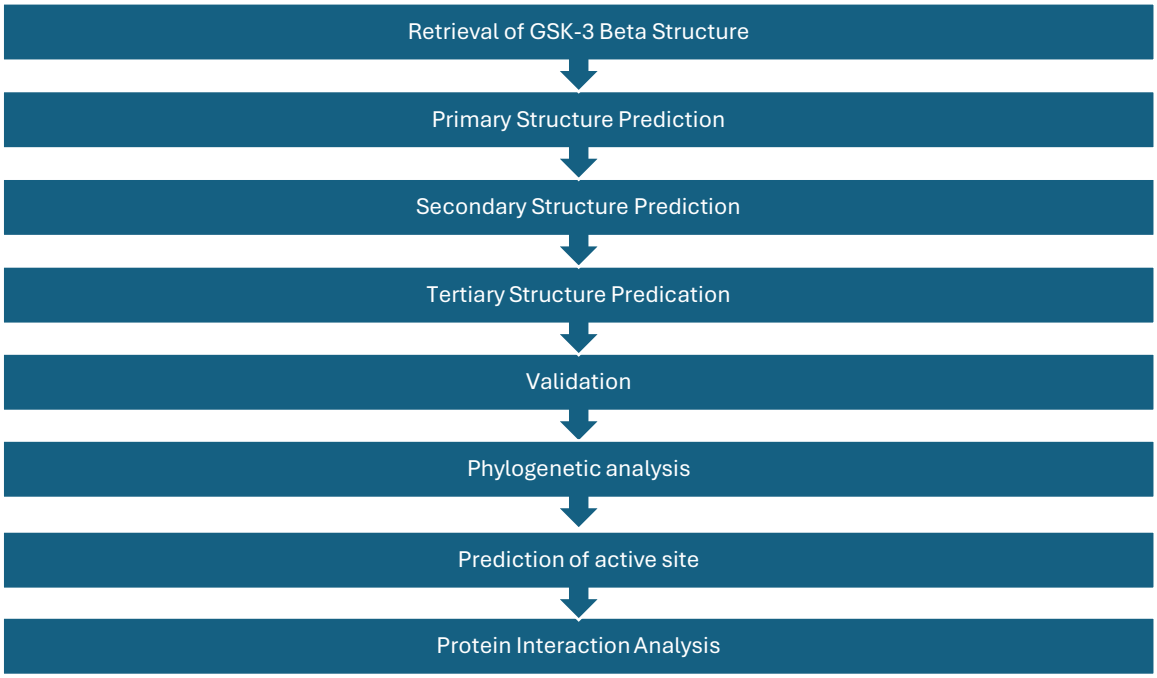

Fig 1. Diagrammatic chronological representation of tools used, and operations performed.

Journal of Chemical Health Risks

www.jchr.org

JCHR (2025) 15(3), 2601-2618 | ISSN:2251-6727

Protein structure and sequence recovery

The structure and FASTA format of the GSK-3 Beta protein (1MQB) were retrieved from the Protein Data Bank (PDB) (https://www.rcsb.org/) for various computational analyses. Protein Data Bank is the single worldwide archive of experimentally determined macromolecular structure data [9].

ProtParam tool for primary sequence analysis

The ExPasy ProtParam (http://web.expasy.org/protparam/) tool was used to analyse the physiochemical parameters of the selected protein. ProtParam computes various Physicochemical properties that can be deduced from a protein sequence. The parameters computed by ProtParam include the molecular weight, theoretical pI, amino acid composition, atomic composition, extinction coefficient, estimated half-life, instability index, aliphatic index, and grand average of hydropathicity (GRAVY).

Prediction of secondary structure

SOPMA (self-optimized prediction method with alignment) (https://npsa-prabi.ibcp.fr/cgi-bin/npsa_automat.pl?page=/NPSA/npsa_sopma.html) was used to predict the secondary structure of GSK-3 Beta. SOPMA accurately predicted the number of random coils, ß-sheet/extended strand, and α-helix conformations in the secondary structure [10].

3D structure prediction and analyses

Comparative homology modelling was performed using the SWISS-MODEL (https://swissmodel.expasy.org) based on automated comparative 3D modelling of protein structures.

Model evaluation

The most crucial step in homology modelling is model evaluation, which demonstrates that the modelled protein is of acceptable quality. Here, the predicted model was evaluated and verified by PROCHECK (https://www.ebi.ac.uk/thorntonsrv/software/PROCHECK/). The PROCHECK suite of programs provides a detailed check on the stereochemistry of a protein structure [11].

Phylogenetic tree construction

For a better understanding of evolutionary relationships, phylogenetic trees were constructed with the help of T-COFFEE (https://tcoffee.crg.eu) software followed by the Neighbour-joining method.

Active site determination

The active site of the protein was determined by the computed atlas of surface topography of proteins (CASTp) (http://sts.bioe.uic.edu/castp/index.html?2r7g). Computed Atlas of Surface Topography of Proteins (CASTp) provides an online resource for locating, delineating, and measuring concave surface regions on three-dimensional structures of proteins. These include pockets located on protein surfaces and voids buried in the interior of proteins. The measurement includes the area and volume of pocket or void by the solvent-accessible model (Richards' surface) and by the molecular surface model (Connolly's surface), all calculated analytically [12].

Phosphorylation site prediction

In our study, phosphorylation sites were identified and verified using the widely respected NetPhos server (https://services.healthtech.dtu.dk/services/NetPhos-3.1/) software, ensuring reliable analysis of protein phosphorylation dynamics. The NetPhos 3.1 server predicts serine, threonine, or tyrosine phosphorylation sites in eukaryotic proteins using ensembles of neural networks.

Protein-Protein Interaction Network Analysis

To analyse the protein-protein interaction network of GSK-3 Beta in lung cancer, we utilized the STRING (Search Tool for the Retrieval of Interacting Genes/Proteins) database version 11.5 (https://string-db.org/). STRING is a comprehensive resource that predicts protein-protein interactions based on known and predicted associations derived from various sources including experimental data, computational prediction methods, and public text collections.

Journal of Chemical Health Risks

www.jchr.org

JCHR (2025) 15(3), 2601-2618 | ISSN:2251-6727

Result and Discussion: -

Physicochemical characterization

Table 1 Physiochemical characterization of protein sequences of GSK-3 Beta as revealed by ProtParam.

S.No.	Accession number	No. Of Amino Acids	MW	PI	(ASP+GLU)	(ARG+LYS)	Ext. Coefficient	Aliphatic Index (Ai)	Instability Index (Ii)	Grand Average of Hydropathicity (Gravy)
1.	1I09	420	46744.34	8.98	41	50	38320	81.05	29.32	-0.319
2.	4PTC_A	441	49229.94	8.89	42	50	39810	78.07	30.40	-0.378
3.	4ACC_A	465	52003.97	8.79	44	51	44280	76.56	30.50	-0.406
4.	1PYX_A	422	46898.51	8.98	41	50	38320	80.66	29.05	-0.322
5.	AAA66475	420	46768.32	8.98	41	50	38320	80.12	28.99	-0.335
6.	1Q3D_A	424	47024.61	8.98	41	50	38320	81.20	28.55	-0.319
7.	5OY4_A	420	46692.50	8.99	41	50	36830	81.05	29.27	-0.315
8.	4J1R_A	424	46990.79	8.99	41	50	36830	80.28	30.12	-0.320
9.	3SAY_A	430	48031.90	8.91	42	50	36830	80.07	28.65	-0.367
10.	5T31_A	420	46706.52	8.99	41	50	36830	81.05	29.27	-0.315

The analysis of the GSK-3 Beta protein sequence 1I09 reveals several key physicochemical properties that are pertinent to its role in lung cancer. The molecular weight of 46,744.34 Da and its composition of 420 amino acids align with typical GSK-3 Beta proteins, establishing 1I09 as a representative sample. The theoretical isoelectric point (pI) of 8.98 suggests that the protein is predominantly positively charged at physiological pH, which may influence its interactions with negatively charged molecules, such as nucleic acids or

Journal of Chemical Health Risks
www.jchr.org
JCHR (2025) 15(3), 2601-2618 | ISSN:2251-6727

phospholipids, potentially impacting cellular signalling pathways crucial in cancer progression.

The stability and solubility of 1I09 are highlighted by its instability index of 29.32 and a GRAVY score of -0.319. The instability index classifies the protein as stable, implying it is likely to remain structurally intact and functional in the cellular environment, which is vital for its role in long-term cellular processes and signalling involved in cancer [13]. The negative GRAVY value indicates hydrophilicity, suggesting that the protein is well-suited for interactions in the aqueous cytoplasmic environment, further supporting its functional relevance in intracellular signalling pathways [14]. Additionally, the high aliphatic index of 81.05 points to considerable thermal stability, enhancing the protein's robustness under varying physiological conditions, which is crucial for maintaining its activity in the dynamic environment of cancer cells.

These physicochemical properties collectively imply that the GSK-3 Beta protein 1I09 is not only structurally stable and functionally versatile but also well-equipped to engage in significant molecular interactions within the cell, making it a pivotal component in the study of lung cancer mechanisms. The comparative consistency of these properties across other GSK-3 Beta sequences reinforces the generalizability of these findings, underlining the importance of GSK-3 Beta proteins in cancer research and potential therapeutic interventions.

Validation

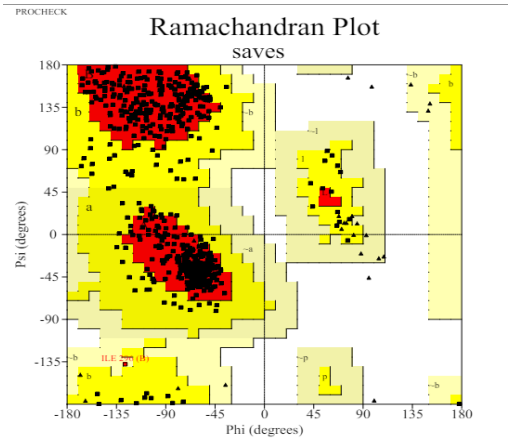

Fig. 2 Ramachandran plot of GSK-3 Beta generated from PROCHECK.

Table 2 Ramachandran plot statistics of the predicted 3d model for the target protein GSK-3 Beta.

Ramachandran Plot Statistics	Number Of Aa Residues	Percentage (%)
Residues in most favoured regions [A,B,L]	487	83.8%
Residues in additional allowed regions [a,b,l,p]	93	16.0%
Residues in generously allowed regions [~a,~b,~l,~p]	1	0.2%
Residues in disallowed regions	0	0.0%
Number of non-glycine and non-proline residues	581	100.0%
Number of end-residues (excl. Gly and Pro)	14	
Number of glycine residues (shown as triangles)	34	
Number of proline residues	50	
Total number of residues	679	

The analysis reveals that 83.8% of the residues are in the most favoured regions, highlighting that the majority of the protein adopts stable and energetically favourable conformations. This high percentage indicates that the GSK-3 Beta protein has a well-folded structure with minimal steric clashes, essential for its functional role in cellular signalling pathways. Additionally, 16.0% of the residues fall within the additional allowed regions,

Journal of Chemical Health Risks
www.jchr.org
JCHR (2025) 15(3), 2601-2618 | ISSN:2251-6727

supporting the protein's necessary flexibility for dynamic functions such as molecular interactions and conformational changes during signal transduction processes.

Only 0.2% of the residues are located in the generously allowed regions, and there are no residues in the disallowed regions. The absence of residues in the disallowed regions underscores the structural reliability and quality of the protein model, suggesting that it lacks significant steric hindrance or unfavourable interactions that could compromise its stability [15]. The presence of 34 glycine and 50 proline residues, which contribute to specific conformational properties, indicates regions of flexibility and rigidity that are essential for the protein's functional diversity.

The high structural integrity and stability implied by the Ramachandran plot results are critical for the GSK-3 Beta protein's function in lung cancer. GSK-3 Beta is involved in various signalling pathways that regulate cell proliferation, apoptosis, and differentiation—processes that are often dysregulated in cancer [16]. A well-folded and stable GSK-3 Beta protein ensures reliable performance in these pathways, potentially influencing the progression of lung cancer [17].

The flexibility and rigidity in specific regions of the protein, as indicated by the presence of glycine and proline residues, may play a pivotal role in the protein's ability to interact with different cellular components and adapt to various functional demands [18]. This adaptability is crucial in the context of cancer, where signalling pathways can be highly dynamic. The absence of disallowed residues further supports the protein's suitability for therapeutic targeting, as it suggests a lower likelihood of aberrant conformations that could lead to dysfunctional signalling [19].

Prediction of secondary structure

Predicting a protein's secondary structure is essential for comprehending its three-dimensional folding. The primary protein sequence is used to predict this secondary structure. SOPMA analysis indicated that random coils dominate the secondary structure of the protein sequences, accounting for over 40%. The data is represented in graphical form mentioning the secondary state rates.

Table 3 Secondary structure prediction using SOPMA analysis.

Parameters	**Score**
Window width	17
Threshold	8
Division factor	5
Helix	0.5970
Sheet	0.9710
Turn	1.5730
Coil	0.7740
Number of proteins in sub database	511

Table 4 Different secondary structure rates (alpha helix, beta sheet, turn and coil), scores and percentage.

Secondary state rates	**Score**	**Percentage**
Alpha helix	129	30.71%
Beta sheet	67	15.95%
Turn	35	8.33%
Coil	189	45.00%

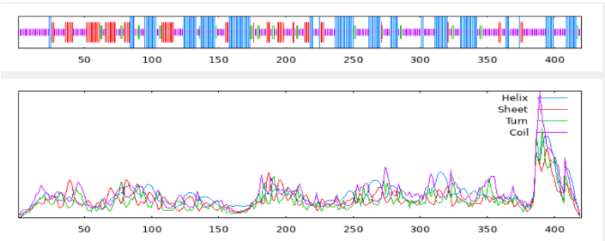

Fig. 3 Graph representation of different secondary state rates and its scores.

The SOPMA (Self-Optimized Prediction Method with Alignment) analysis of the GSK-3 Beta protein provides a comprehensive overview of its secondary structure, which is crucial for understanding its functional roles, particularly in lung cancer. According to the analysis, random coils dominate the secondary structure of the GSK-3 Beta protein, accounting for 45% of the protein. This high percentage of random coils indicates significant regions of conformational flexibility within the protein. Such flexibility is essential for GSK-3 Beta's

Journal of Chemical Health Risks
www.jchr.org
JCHR (2025) 15(3), 2601-2618 | ISSN:2251-6727

ability to interact with a wide variety of substrates and regulatory proteins [20].

The analysis further reveals that alpha helices make up 30.71% of the GSK-3 Beta structure, with a score of 0.5970. Alpha helices are known for their role in providing structural stability and facilitating protein-protein interactions. The substantial proportion of alpha helices suggests that these regions are integral to maintaining the protein's stability and function [21]. This structural feature is particularly important for GSK-3 Beta's role in signalling pathways, where stable and specific interactions are necessary for effective signal transduction. Beta sheets, which constitute 15.95% of the protein and have a score of 0.9710, also contribute significantly to the protein's structural integrity. Beta sheets form the core structural elements that provide stability and rigidity, facilitating the formation of stable interfaces for protein-protein and protein-ligand interactions [22].

Turns, which connect elements of secondary structure such as alpha helices and beta sheets, account for 8.33% of the GSK-3 Beta protein and have a score of 1.5730. These turn regions are crucial for the protein's overall three-dimensional folding, allowing it to assume its functional conformation. The presence of turns highlights their importance in connecting the structural elements and contributing to the protein's compact and functional three-dimensional structure [23]. This balanced composition of alpha helices, beta sheets, and turns ensures that GSK-3 Beta maintains its functional conformation while being versatile enough to participate in dynamic cellular processes.

The graphical representation of the SOPMA analysis visually corroborates these findings, emphasizing the dominance of random coils and the balanced presence of alpha helices and beta sheets. The graph quantifies the proportions of each type of secondary structure, highlighting the significant flexibility and stability within GSK-3 Beta's conformation. This structural adaptability is crucial for GSK-3 Beta's involvement in oncogenic processes, where precise regulatory functions and interactions with various molecular partners are essential [24]. Understanding these structural features enhances our comprehension of GSK-3 Beta's role in lung cancer, providing insights that could guide the development of targeted therapeutic strategies aimed at modulating its activity within cancer cells.

Prediction of active sites

Table 5 Different active sites prediction using Castp.

PocID	Area (SA) Å^2	Volume (SA) Å^3
1	2102.539	3237.680
2	1040.389	841.037
3	346.792	436.876
4	79.062	71.900
5	172.717	66.164
6	92.976	52.203
7	71.076	35.001
8	79.473	34.818
9	53.551	26.760
10	56.430	25.603

Table 6 Active sites (5) with different atoms (CA, O, CD1, CE1, CZ).

PocID	Chain	SeqID	AA	Atom
1	A	140	TYR	CA
1	A	140	TYR	O
1	A	140	TYR	CD1

Journal of Chemical Health Risks
www.jchr.org
JCHR (2025) 15(3), 2601-2618 | ISSN:2251-6727

1	A	140	TYR	CE1
1	A	140	TYR	CZ

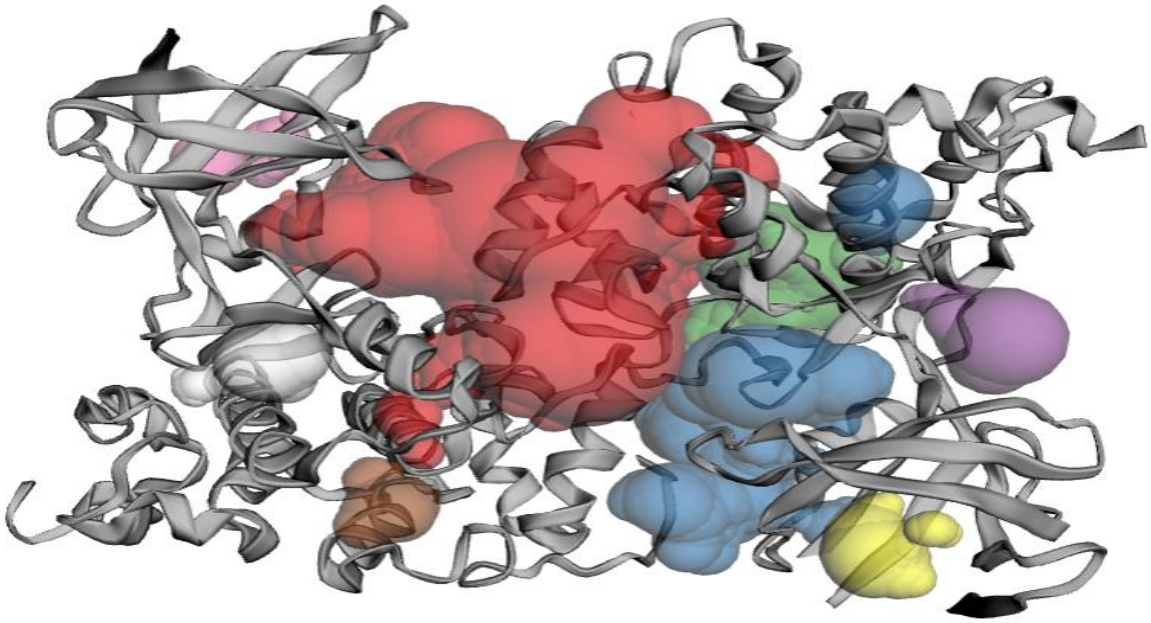

Fig. 4 Predicted model having different active sites represented by different colours.

The CASTp (Computed Atlas of Surface Topography of proteins) analysis of GSK-3 Beta (Glycogen Synthase Kinase 3 beta) provided valuable insights into the protein's structural characteristics, including detailed information on pocket IDs, their corresponding surface areas, and volumes, which are crucial for understanding the protein's structure-function relationship.

The analysis reveals several pockets on the GSK-3 Beta protein, with Pocket 1 standing out due to its large surface area (2102.539 Å²) and volume (3237.680 Å³). This suggests that Pocket 1 might be the primary active site or a significant allosteric site, potentially influencing the protein's activity. Notably, this pocket includes multiple atoms from Tyrosine (TYR) at position 140 on chain A, indicating critical points for binding interactions. Tyrosine's aromatic ring and potential for π-π interactions make it significant for binding various ligands.

Pocket 2, with a surface area of 1040.389 Å² and volume of 841.037 Å³, is the second largest and could also play an important role in ligand binding or protein-protein interactions. Smaller pockets, such as Pocket 3 (surface area of 346.792 Å² and volume of 436.876 Å³) and others ranging from Pocket 4 to Pocket 10, while less significant in size, may still be relevant for binding smaller molecules or ions.

Understanding these pockets and their properties aids in multiple aspects of lung cancer research. For instance, identifying significant pockets like Pocket 1 and Pocket 2 can facilitate the design of inhibitors or activators targeting GSK-3 Beta, potentially modulating its activity in lung cancer. Insights into these binding sites also enhance the understanding of how GSK-3 Beta interacts with other molecules, influencing signalling pathways involved in lung cancer progression. Furthermore, detailed knowledge of key binding sites allows for targeted studies on how mutations might alter binding site geometry or function, contributing to cancer development or progression [25].

The high-resolution images provided, with dimensions of 1920 x 1080 in true colour are useful for detailed structural analysis and visualization, further supporting the interpretation of these findings. Overall, this CASTp analysis offers a comprehensive understanding of the potential binding sites on GSK-3 Beta, highlighting the importance of focusing on the largest pockets for

Journal of Chemical Health Risks
www.jchr.org
JCHR (2025) 15(3), 2601-2618 | ISSN:2251-6727

significant insights into targeting this protein in lung cancer therapy [26]. Further in silico and experimental validation would enhance the application of these findings, paving the way for potential therapeutic advancements.

Phylogenetic analysis

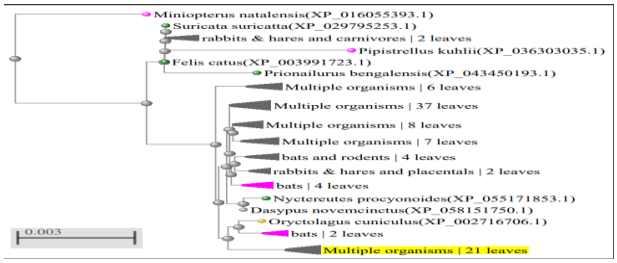

Fig. 5 Phylogenetic analysis using (A) Fast minimum evolution and (B) Neighbour joining methods for the protein GSK-3 Beta.

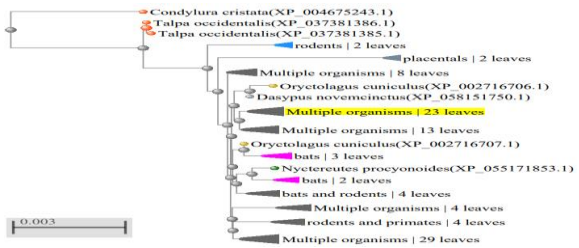

The phylogenetic analysis of the GSK-3 Beta protein, depicted in the obtained phylogenetic tree diagram, reveals detailed insights into the evolutionary relationships among various homologous proteins across different species. This diagram illustrates the evolutionary pathways and distances between the sequences, highlighting both conserved and divergent features of the GSK-3 Beta protein. By examining the branching patterns and lengths of the branches, we can infer the relative evolutionary distances and the degree of relatedness between different sequences [27].

The phylogenetic tree shows multiple branches, each representing different species or homologous GSK-3 Beta proteins. Nodes where branches converge represent common ancestors, indicating points of evolutionary divergence. The length of the branches is indicative of the evolutionary distance, with shorter branches representing more closely related sequences and longer branches indicating more significant divergence. This detailed visualization allows us to identify clusters of closely related sequences, suggesting high similarity and potentially conserved functions within these clusters.

One significant implication of the phylogenetic tree is the identification of conserved regions within the GSK-3 Beta protein. Sequences that are closely grouped in the tree are likely to share conserved functional domains that are critical for the protein's regulatory roles. These conserved domains are essential for maintaining the structural integrity and functional capabilities of GSK-3 Beta. Understanding these conserved regions is crucial for lung cancer research, as they can be targeted for therapeutic interventions aimed at modulating GSK-3 Beta's activity in cancer cells [28]. Specifically, conserved regions may play vital roles in the pathways that control cell proliferation and apoptosis, processes that are often dysregulated in lung cancer.

Moreover, the phylogenetic tree highlights evolutionary divergence among the GSK-3 Beta proteins. The longer branches and more distantly related sequences suggest functional diversification or species-specific adaptations [29]. These variations can provide insights into how different species have evolved unique mechanisms involving GSK-3 Beta. By comparing the conserved and divergent regions, researchers can identify specific functional motifs that are critical for GSK-3 Beta's role in lung cancer. For instance, evolutionary changes in the protein that are unique to humans or closely related species may help pinpoint mechanisms specific to human lung cancer pathogenesis [30]. This can guide the development of targeted therapies that consider these evolutionary differences, ensuring treatments are effective for human-specific regulatory pathways.

Tertiary structure prediction

Table 7 Predicted protein model quality estimation by SWISS-MODEL**.**

Parameters	**Score**
MolProbity Score	1.02
Clash Score	0
Ramachandran Favoured	90.9

Journal of Chemical Health Risks

www.jchr.org

JCHR (2025) 15(3), 2601-2618 | ISSN:2251-6727

	1 %
Ramachandran Outliers A406 GLY, A419 SER, A11 ALA, A402 THR, A258 PRO, A414 ALA, A413 SER, A9 SER, A 395 THR, A410 ASN, A417 SER, A399 ASP, A411 ALA, A407 GLN, A416 ALA	3. 59 %
Rotamer Outliers A408 THR, A402 THR	0. 55 %
C-Beta Deviations A420 THR, A419 SER, A395 THR, A413 SER, A399 ASP, A417 SER, A124 ASP, A200 ASP, A218 CYS	9
Bad Bonds A301 TRP	1 / 33 69
Bad Angles (A414 ALA-A415 SER), (A411 ALA-A412 ALA), (A417 SER-A418 ASN), A124 ASP, (A403 GLY-A404 ASP), (A371 PRO-A372 PRO), A355 ASP, A301 TRP, A402 THR, A413 SER, (A390 THR-A391 PRO), A395 THR, A93 PHE, A420 THR, A145 HIS, (A43 THR-A44 PRO), (A153 LEU-A154 PRO), A381 HIS, (A408 THR-A409 ASN), A179 HIS, (A299 HIS-A300 PRO), A330 THR, (A183 LYS-A184 PRO), (A135 VAL-A136 PRO), A419 SER, A337 HIS, (A310 PRO-A311 PRO), (A324 THR-A325 PRO), (A416 ALA-A417 SER), (A275 THR-A276 PRO), A106 HIS, A396 ALA, (A330 THR-A331 PRO)	38 / 45 81
Cis non-proline (A403 GLY-A404 ASP), (A411 ALA-A412 ALA), (A414 ALA-A415 SER), (A417 SER-A418 ASN)	4 / 38 8
Twisted non-proline (A395 THR-A396 ALA), (A398 SER-A399 ASP), (A399 ASP-A400 ALA), (A406 GLY-A407 GLN), (A407 GLN-A408 THR), (A409 ASN-A410 ASN), (A410 ASN-A411 ALA), (A412 ALA-A413 SER), (A413 SER-A414 ALA), (A415 SER-A416 ALA), (A418 ASN-A419 SER)	11 / 38 8

The SWISS-MODEL analysis of GSK-3 Beta offers a comprehensive assessment of the protein's structural quality, crucial for elucidating its role in lung cancer. This analysis evaluates various parameters that collectively indicate the model's reliability and highlights potential areas for further refinement. Firstly, the MolProbity score of 1.02 is indicative of a high-quality model characterized by low steric clashes and excellent geometry. Scores below 2.0 are generally considered top-notch, suggesting that this model of GSK-3 Beta is highly accurate [31]. Additionally, the clash score of 0.00 underscores the model's robustness, indicating no steric clashes between atoms, which implies an ideal fit with no physical overlaps [32]. This is highly favorable for ensuring the model's precision and reliability in subsequent analyses.

Furthermore, the Ramachandran favored percentage of 90.91% indicates that the majority of the amino acid residues in GSK-3 Beta are positioned in the favored regions of the Ramachandran plot. This is a strong indicator of good stereochemical quality, as values exceeding 90% typically reflect a reliable model [33]. However, the presence of 3.59% of residues as Ramachandran outliers suggests that there are areas within the protein that might require further refinement or are regions with unique structural conformations that need closer examination. These outliers, which include residues such as GLY A406 and SER A419, might play significant roles in the protein's function or interactions with other molecules.

The analysis also highlights a low percentage of rotamer outliers, with only 0.55% of residues adopting energetically unfavorable conformations. This is indicative of the model's overall reliability, as most side chains are in favorable conformations [34]. However, nine C-beta deviations are noted, which suggest minor local distortions in the protein's structure that might need attention during further model optimization. These deviations include residues like THR A420 and ASP A124, which could be critical for maintaining the protein's stability and function.

Another aspect of the model's assessment involves evaluating bad bonds and angles. The analysis identifies only one bad bond (TRP A301 out of 3369), which indicates that the bond lengths are predominantly within acceptable ranges, contributing to the model's overall

Journal of Chemical Health Risks
www.jchr.org
JCHR (2025) 15(3), 2601-2618 | ISSN:2251-6727

structural accuracy [35]. However, there are 38 bad angles out of 4581, which might suggest areas needing refinement but are not necessarily detrimental if they correspond to functional regions that require flexibility. These bad angles are distributed across various residues such as A414 ALA-A415 SER and A179 HIS, which might indicate localized regions of strain or conformational uniqueness.

Additionally, the model includes four cis non-proline peptides and eleven twisted non-proline peptides. Cis conformations in non-proline residues are rare and may indicate regions with unusual structural properties or areas that might need further examination. Twisted peptides could suggest regions with strained conformations, potentially impacting the protein's stability or function [36]. These structural peculiarities, involving residues like A403 GLY-A404 ASP and A418 ASN-A419 SER, might be critical for the protein's functionality and its interactions in a cellular environment.

The high-quality SWISS-MODEL of GSK-3 Beta, characterized by its excellent MolProbity and clash scores, provides a reliable structural framework for in silico studies. The few noted outliers and deviations highlight areas for targeted refinement or special functional significance, such as potential binding sites or mutation hotspots [37]. Understanding these structural nuances is vital for designing inhibitors or modulators that target GSK-3 Beta in lung cancer therapy. For instance, areas with high-quality geometry can be prioritized for drug binding studies, while outlier regions might be investigated for their role in disease-specific mutations or unique functional adaptations.

Structure estimation

Table 8 Predicted five models using I-TASSER analysis.

Name	C-score	Exp.TM-Score	Exp. RMSD	No. of decoys	Cluster density
Model1:	-0.70	0.62+-0.14	8.5+-4.5	2023	0.1522
Model2:	-2.36			431	0.0291
Model3:	-3.81			109	0.0068
Model4:	-2.66			307	0.0216
Model5:	-3.43			133	0.0099

The C-score is a confidence score used to assess the quality of predicted models by I-TASSER. It is determined based on the significance of threading template alignments and the convergence parameters from structure assembly simulations. C-score is typically in the range of [-5,2], where a C-score of higher value signifies a model with a high confidence and vice-versa [38].

TM-score and RMSD are known standards for measuring structural similarity between two structures which are usually used to measure the accuracy of structure modeling when the native structure is known [39].

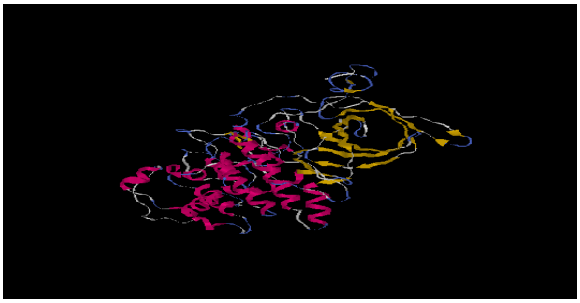

Fig. 6 (a) Model 1 having C-score of-0.70

Model 1 (Figure 6) exhibits the highest confidence among the predicted structures, reflected by its C-score of -0.70. The C-score is a crucial indicator, as it estimates the model's reliability based on the quality of the threading template alignments and the structural assembly simulations' convergence. A C-score closer to 2 denotes higher confidence [40]. Although -0.70 is not

Journal of Chemical Health Risks
www.jchr.org
JCHR (2025) 15(3), 2601-2618 | ISSN:2251-6727

extremely high, it suggests that Model 1 is reasonably reliable. The Exp. TM-score of 0.62 ± 0.14 further reinforces this, as a TM-score above 0.5 typically indicates a model with a correct topology. The RMSD of 8.5 ± 4.5 Å provides insight into the average distance between atoms of superimposed proteins, indicating moderate deviation from the native structure [41]. The large number of decoys (2023) and the highest cluster density (0.1522) among the models suggest extensive and consistent sampling, making Model 1 the most reliable for further analysis.

(b) Model 2 having C-score of -2.36

Model 2 (Figure 7), with a C-score of -2.36, is significantly less reliable than Model 1. The C-score indicates a lower confidence level, suggesting that the predicted structure is less likely to be accurate. The number of decoys (431) is considerably fewer than in Model 1, indicating less extensive sampling, which can lead to a less reliable model [42]. The cluster density of 0.0291 is also much lower, reflecting less consistency among the decoys. This lack of convergence and sampling reliability is why Model 2 lacks Exp. TM-score and Exp. RMSD values, as these metrics would not be meaningful or reliable for such a low-confidence model.

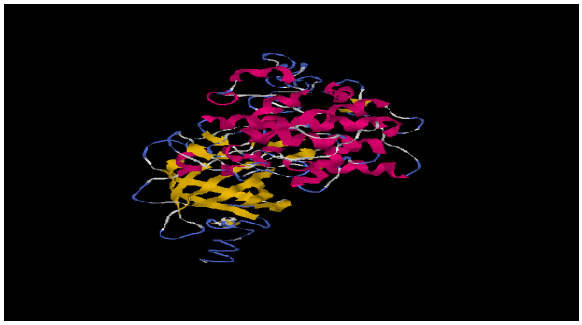

(c) Model 3 having C-score of -3.81

Model 3 (Figure 8) has the lowest C-score of -3.81, indicating very low confidence in the predicted structure. With only 109 decoys, this model has the least extensive sampling, and the cluster density of 0.0068 is the lowest among all models, suggesting very poor convergence. These factors contribute to the model's low reliability, making it unsuitable for detailed structural analysis or functional studies [43]. The absence of Exp. TM-score and Exp. RMSD further emphasizes the lack of confidence in this model.

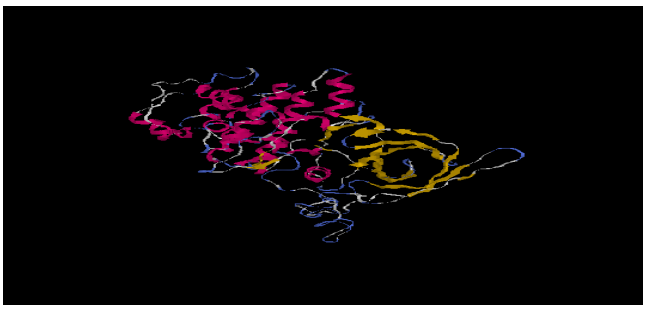

(d) Model 4 having C-score of -2.66

Model 4 (Figure 9), with a C-score of -2.66, also indicates low confidence in the predicted structure. The model has 307 decoys, which is more than Model 3 but still significantly less than Model 1. The cluster density of 0.0216 shows some degree of convergence, but it remains too low to inspire confidence in the model's accuracy. As with Models 2 and 3, the lack of Exp. TM-score and Exp. RMSD metrics highlight the low reliability and the likely inaccuracy of this predicted structure.

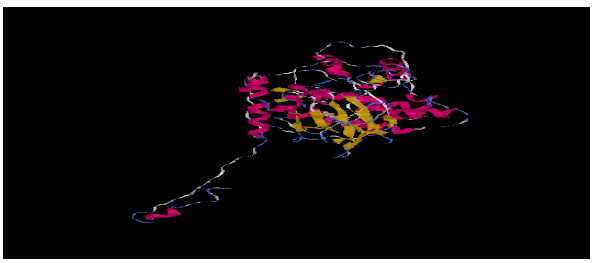

(e) Model 5 having C-score of -3.43

Model 5 (Figure 10), with a C-score of -3.43, is another low-confidence model. The number of decoys (133) and the cluster density (0.0099) indicate poor sampling and

Journal of Chemical Health Risks
www.jchr.org
JCHR (2025) 15(3), 2601-2618 | ISSN:2251-6727

low structural convergence. This low confidence and poor structural reliability make the model inadequate for detailed functional analysis. The absence of Exp. TM-score and Exp. RMSD values further confirm that Model 5 is not reliable.

Model 1, with its higher confidence and detailed structural metrics, is the most suitable for further analysis. It can help identify potential binding sites for inhibitors or drugs that can modulate GSK-3 Beta activity, providing a foundation for designing targeted therapies. Models 2-5, due to their low confidence scores and lack of detailed metrics, are less reliable and should be approached with caution in any functional studies. These models underscore the importance of relying on high-confidence predictions when developing therapeutic strategies for lung cancer.

Protein-Protein Interaction Network Analysis

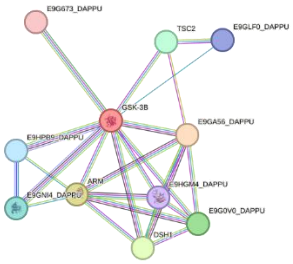

Fig. 7 Map of the protein-protein interaction of GSK-3 Beta protein using STRING.

Predicted functional parameters

Table 9 Predicted interacting protein partners of the query sequence from STRING server.

Accession Number	Protein Name	Score
E9GA56_DAPPU	Uncharacterized protein	0.999
ARM	Putative transcription coactivator armadillo	0.998
DSH1	Disheveled-like protein	0.975
E9GOVO_DAPPU	Uncharacterized protein	0.973
TSC2	Putative tuberous sclerosis 2 isoform 3-like protein	0.965
E9GNI4_DAPPU	Uncharacterized protein; Belongs to the protein kinase superfamily	0.957
E9HPB9_DAPPU	Uncharacterized protein	0.957
E9GLFO_DAPPU	Rab-GAP TBC domain-containing protein	0.900
E9HGM4_DAPPU	Protein kinase domain-containing protein; Belongs to the protein kinase superfamily	0.897
E9G673_DAPPU	PPM-type phosphatase domain-containing protein	0.878

Table 10 Analysis result of GSK-3 Beta showcasing nodes, edges and p-value.

Network stats	Score
Number of nodes	21
Number of edges	86
Average node degree	8.91
Avg. local clustering coefficient	0.796
Expected number of edges	23
PPI enrichment p-value	< 1.0e-16

The STRING results give a comprehensive overview of the interaction network involving GSK-3 Beta in lung cancer, focusing on predicted functional partners, network statistics, and the overall interaction enrichment. The predicted functional partners of GSK-3 Beta include several proteins with high interaction scores, indicating strong confidence in these predicted interactions [44]. The top interactions are with proteins such as E9GA56_DAPPU (an uncharacterized protein), ARM (a putative transcription coactivator armadillo), and DSH1 (a dishevelled-like protein), all with scores above 0.97.

Journal of Chemical Health Risks

www.jchr.org

JCHR (2025) 15(3), 2601-2618 | ISSN:2251-6727

These high scores suggest that these proteins have a significant likelihood of interacting with GSK-3 beta [45]. ARM and DSH1, in particular, are known to play critical roles in signal transduction pathways, notably the Wnt signalling pathway, which is crucial in various cancers, including lung cancer. The inclusion of uncharacterized proteins and those belonging to different families, such as protein kinases and phosphatases, indicates that GSK-3 Beta is potentially involved in a wide array of cellular processes [46].

The network statistics provide valuable insights into the structure and robustness of the predicted protein-protein interaction (PPI) network. The network consists of 21 nodes and 86 edges, with an average node degree of 8.91, indicating that each protein in the network interacts with approximately nine other proteins on average. This high degree of connectivity suggests a highly interactive network [47]. Additionally, the average local clustering coefficient is 0.796, reflecting the tendency of proteins to form tightly knit clusters within the network. This high clustering coefficient implies that GSK-3 Beta and its interaction partners form a robust and closely interconnected group of proteins. The expected number of edges, based on random chance, is 23, significantly lower than the observed 86 edges. This substantial difference, coupled with a PPI enrichment p-value of less than 1.0e-16, indicates that the observed interactions are highly significant and not due to random chance [48]. This statistical significance underscores the biological relevance of the interactions and supports the hypothesis that GSK-3 Beta plays a crucial role in lung cancer through its interaction network.

The detailed analysis of the STRING results suggests that GSK-3 Beta is potentially a central player in a complex and highly interconnected PPI network in lung cancer. The high-confidence interactions with key signalling molecules, such as those involved in the Wnt signalling pathway, underscore its critical role in cancer-related pathways. The diverse range of interacting proteins, including uncharacterized ones, highlights the multifaceted nature of GSK-3 Beta's involvement in cellular processes [49]. The robust network structure, indicated by the high node degree and clustering coefficient, further emphasizes the importance of GSK-3 Beta and its partners in maintaining cellular integrity and function in lung cancer [50]. The highly significant PPI enrichment reinforces the idea that GSK-3 Beta is not only involved in numerous interactions but that these interactions are biologically meaningful and crucial for understanding the molecular mechanisms of lung cancer.

Conclusion

Our comprehensive in silico analysis of Glycogen Synthase Kinase 3 beta (GSK-3 Beta) provides significant insights into its structural and functional attributes, shedding light on its implications in lung cancer. Our study leveraged advanced computational tools to analyse GSK-3 Beta's physicochemical properties, secondary structure, three-dimensional modelling, and active site characteristics, revealing its stability and functionality within the cellular environment.

Our findings highlight GSK-3 Beta's stability, flexibility, and structural integrity, which are crucial for its role in intracellular signalling pathways [51]. The identification of a promising active site pocket suggests a potential target for therapeutic intervention, aligning with current research efforts aimed at developing GSK-3 Beta inhibitors for cancer therapy [52].

GSK-3 Beta's involvement in critical pathways such as Wnt/β-catenin, PI3K/AKT, and NF-κB makes it a key player in the pathogenesis of lung cancer [53]. Our in silico analysis provides a detailed structural framework that can be leveraged to design targeted inhibitors, offering a potential therapeutic strategy to modulate GSK-3 Beta activity in lung cancer treatment.

While our study provides substantial insights, experimental validation is crucial to confirm these findings. Future research should focus on biochemical and cellular assays to validate the predicted active sites and assess the efficacy of potential inhibitors. Additionally, exploring the interaction dynamics of GSK-3 Beta with other cellular proteins involved in lung cancer could reveal further therapeutic targets [54].

Our study demonstrates the power of in silico approaches in accelerating the discovery and development of targeted treatments, paving the way for more effective lung cancer therapies. Future research should focus on the experimental validation of these computational findings and the exploration of GSK-3 Beta inhibitors as

Journal of Chemical Health Risks

www.jchr.org

JCHR (2025) 15(3), 2601-2618 | ISSN:2251-6727

potential therapeutic agents, ultimately contributing to the advancement of personalized medicine in oncology.

References

[1] Brown JS, Amend SR, Austin RH, Gatenby RA, Hammarlund EU, Pienta KJ. Updating the Definition of Cancer. Mol Cancer Res. 2023 Nov 1;21(11):1142-1147. doi: 10.1158/1541-7786.MCR-23-0411. PMID: 37409952; PMCID: PMC10618731.

[2] Anand P, Kunnumakkara AB, Sundaram C, Harikumar KB, Tharakan ST, Lai OS, Sung B, Aggarwal BB. Cancer is a preventable disease that requires major lifestyle changes. Pharm Res. 2008 Sep;25(9):2097-116. doi: 10.1007/s11095-008-9661-9. Epub 2008 Jul 15. Erratum in: Pharm Res. 2008 Sep;25(9):2200. Kunnumakara, Ajaikumar B [corrected to Kunnumakkara, Ajaikumar B]. PMID: 18626751; PMCID: PMC2515569.

[3] Dela Cruz CS, Tanoue LT, Matthay RA. Lung cancer: epidemiology, etiology, and prevention. Clin Chest Med. 2011 Dec;32(4):605-44. doi: 10.1016/j.ccm.2011.09.001. PMID: 22054876; PMCID: PMC3864624.

[4] Alves M, Borges DP, Kimberly A, Martins Neto F, Oliveira AC, de Sousa JC, Nogueira CD, Carneiro BA, Tavora F. Glycogen Synthase Kinase-3 Beta Expression Correlates With Worse Overall Survival in Non-Small Cell Lung Cancer-A Clinicopathological Series. Front Oncol. 2021 Mar 9;11:621050. doi: 10.3389/fonc.2021.621050. PMID: 33767989; PMCID: PMC7985549.

[5] Vanhove, K.; Derveaux, E.; Mesotten, L.; Thomeer, M.; Criel, M.; Mariën, H.; Adriaensens, P. Unraveling the Rewired Metabolism in Lung Cancer Using Quantitative NMR Metabolomics. Int. J. Mol. Sci. 2022, 23, 5602. https://doi.org/10.3390/ijms23105602

[6] Svetlana E. Nikoulina, Theodore P. Ciaraldi, Sunder Mudaliar, Leslie Carter, Kirk Johnson, Robert R. Henry; Inhibition of Glycogen Synthase Kinase 3 Improves Insulin Action and Glucose Metabolism in Human Skeletal Muscle . Diabetes 1 July 2002; 51 (7): 2190–2198. https://doi.org/10.2337/diabetes.51.7.2190

[7] Wang L, Li J, Di LJ. Glycogen synthesis and beyond, a comprehensive review of GSK3 as a key regulator of metabolic pathways and a therapeutic target for treating metabolic diseases. Med Res Rev. 2022 Mar;42(2):946-982. doi: 10.1002/med.21867. Epub 2021 Nov 3. PMID: 34729791; PMCID: PMC9298385.

[8] Sood N, Chaudhary S, Pardeshi T, Mujawar S, Deshmukh KB, Sheikh SA, Sharma P. In-silico study of small cell lung cancer based on protein structure and function: A new approach to mimic biological system. J Adv Pharm Technol Res. 2015 Jul-Sep;6(3):125-9. doi: 10.4103/2231-4040.161513. PMID: 26317077; PMCID: PMC4542399.

[9] Velankar S, Burley SK, Kurisu G, Hoch JC, Markley JL. The Protein Data Bank Archive. Methods Mol Biol. 2021;2305:3-21. doi: 10.1007/978-1-0716-1406-8_1. PMID: 33950382.

[10] Sharifi F, Sharifi I, Babaei Z, Alahdin S, Afgar A. Bioinformatics evaluation of anticancer properties of GP63 protein-derived peptides on MMP2 protein of melanoma cancer. J Pathol Inform. 2023 Jan 12;14:100190. doi: 10.1016/j.jpi.2023.100190. PMID: 36700237; PMCID: PMC9867975.

[11] Laskowski, Roman & Macarthur, M.W. & Moss, D.S. & Thornton, Janet. (1993). PROCHECK: A program to check the stereochemical quality of protein structures. Journal of Applied Crystallography. 26. 283-291. 10.1107/S0021889892009944.

[12] Binkowski TA, Naghibzadeh S, Liang J. CASTp: Computed Atlas of Surface Topography of proteins. Nucleic Acids Res. 2003 Jul 1;31(13):3352-5. doi: 10.1093/nar/gkg512. PMID: 12824325; PMCID: PMC168919.

[13] Wattanathamsan O, Pongrakhananon V. Emerging role of microtubule-associated proteins on cancer metastasis. Front Pharmacol. 2022 Sep 14;13:935493. doi: 10.3389/fphar.2022.935493. PMID: 36188577; PMCID: PMC9515585.

[14] Chang KY, Yang JR. Analysis and prediction of highly effective antiviral peptides based on random

forests. PLoS One. 2013 Aug 5;8(8):e70166. doi: 10.1371/journal.pone.0070166. PMID: 23940542; PMCID: PMC3734225.

[15] Maxwell PI, Popelier PLA. Unfavorable regions in the ramachandran plot: Is it really steric hindrance? The interacting quantum atoms perspective. J Comput Chem. 2017 Nov 5;38(29):2459-2474. doi: 10.1002/jcc.24904. Epub 2017 Aug 25. PMID: 28841241; PMCID: PMC5659141.

[16] Jacobs KM, Bhave SR, Ferraro DJ, Jaboin JJ, Hallahan DE, Thotala D. GSK-3β: A Bifunctional Role in Cell Death Pathways. Int J Cell Biol. 2012;2012:930710. doi: 10.1155/2012/930710. Epub 2012 May 21. PMID: 22675363; PMCID: PMC3364548.

[17] Domoto T, Uehara M, Bolidong D, Minamoto T. Glycogen Synthase Kinase 3β in Cancer Biology and Treatment. Cells. 2020 Jun 3;9(6):1388. doi: 10.3390/cells9061388. PMID: 32503133; PMCID: PMC7349761.

[18] Huber R. Flexibility and rigidity, requirements for the function of proteins and protein pigment complexes. Eleventh Keilin memorial lecture. Biochem Soc Trans. 1987 Dec;15(6):1009-20. doi: 10.1042/bst0151009. PMID: 3502256.

[19] Kumar M, Rathore RS. Disallowed spots in protein structures. Biochim Biophys Acta Gen Subj. 2023 Dec;1867(12):130493. doi: 10.1016/j.bbagen.2023.130493. Epub 2023 Oct 20. PMID: 37865175.

[20] Beurel E, Grieco SF, Jope RS. Glycogen synthase kinase-3 (GSK3): regulation, actions, and diseases. Pharmacol Ther. 2015 Apr;148:114-31. doi: 10.1016/j.pharmthera.2014.11.016. Epub 2014 Nov 27. PMID: 25435019; PMCID: PMC4340754.

[21] Heyden M, Freites JA, Ulmschneider MB, White SH, Tobias DJ. Assembly and Stability of α-Helical Membrane Proteins. Soft Matter. 2012 Aug 14;8(30):7742-7752. doi: 10.1039/C2SM25402F. PMID: 23166562; PMCID: PMC3500387.

[22] Perczel A, Gáspári Z, Csizmadia IG. Structure and stability of beta-pleated sheets. J Comput Chem. 2005 Aug;26(11):1155-68. doi: 10.1002/jcc.20255. PMID: 15952205.

[23] Stollar EJ, Smith DP. Uncovering protein structure. Essays Biochem. 2020 Oct 8;64(4):649-680. doi: 10.1042/EBC20190042. Erratum in: Essays Biochem. 2021 Jul 26;65(2):407. PMID: 32975287; PMCID: PMC7545034.

[24] Hurcombe, J.A., Hartley, P., Lay, A.C. et al. Podocyte GSK3 is an evolutionarily conserved critical regulator of kidney function. Nat Commun **10**, 403 (2019). https://doi.org/10.1038/s41467-018-08235-1

[25] Nishi H, Tyagi M, Teng S, Shoemaker BA, Hashimoto K, Alexov E, Wuchty S, Panchenko AR. Cancer missense mutations alter binding properties of proteins and their interaction networks. PLoS One. 2013 Jun 14;8(6):e66273. doi: 10.1371/journal.pone.0066273. PMID: 23799087; PMCID: PMC3682950.

[26] Balboni B, Tripathi SK, Veronesi M, Russo D, Penna I, Giabbai B, Bandiera T, Storici P, Girotto S, Cavalli A. Identification of Novel GSK-3β Hits Using Competitive Biophysical Assays. Int J Mol Sci. 2022 Mar 31;23(7):3856. doi: 10.3390/ijms23073856. PMID: 35409221; PMCID: PMC8998611.

[27] Stadler PF, Geiß M, Schaller D, López Sánchez A, González Laffitte M, Valdivia DI, Hellmuth M, Hernández Rosales M. From pairs of most similar sequences to phylogenetic best matches. Algorithms Mol Biol. 2020 Apr 9;15:5. doi: 10.1186/s13015-020-00165-2. PMID: 32308731; PMCID: PMC7147060.

[28] Augello G, Emma MR, Cusimano A, Azzolina A, Montalto G, McCubrey JA, Cervello M. The Role of GSK-3 in Cancer Immunotherapy: GSK-3 Inhibitors as a New Frontier in Cancer Treatment. Cells. 2020 Jun 9;9(6):1427. doi: 10.3390/cells9061427. PMID: 32526891; PMCID: PMC7348946.

[29] Yoo MJ, Albert VA, Soltis PS, Soltis DE. Phylogenetic diversification of glycogen synthase kinase 3/SHAGGY-like kinase genes in plants. BMC Plant Biol. 2006 Feb 21;6:3. doi: 10.1186/1471-2229-6-3. PMID: 16504046; PMCID: PMC1524769.

[30] Rifkin RF, Potgieter M, Ramond JB, Cowan DA. Ancient oncogenesis, infection and human evolution. Evol Appl. 2017 Jul 11;10(10):949-964.

Journal of Chemical Health Risks

www.jchr.org

JCHR (2025) 15(3), 2601-2618 | ISSN:2251-6727

doi: 10.1111/eva.12497. PMID: 29151852; PMCID: PMC5680625.

[31] Chen VB, Arendall WB 3rd, Headd JJ, Keedy DA, Immormino RM, Kapral GJ, Murray LW, Richardson JS, Richardson DC. MolProbity: all-atom structure validation for macromolecular crystallography. Acta Crystallogr D Biol Crystallogr. 2010 Jan;66(Pt 1):12-21. doi: 10.1107/S0907444909042073. Epub 2009 Dec 21. PMID: 20057044; PMCID: PMC2803126.

[32] Ramachandran S, Kota P, Ding F, Dokholyan NV. Automated minimization of steric clashes in protein structures. Proteins. 2011 Jan;79(1):261-70. doi: 10.1002/prot.22879. PMID: 21058396; PMCID: PMC3058769.

[33] Sobolev OV, Afonine PV, Moriarty NW, Hekkelman ML, Joosten RP, Perrakis A, Adams PD. A Global Ramachandran Score Identifies Protein Structures with Unlikely Stereochemistry. Structure. 2020 Nov 3;28(11):1249-1258.e2. doi: 10.1016/j.str.2020.08.005. Epub 2020 Aug 27. PMID: 32857966; PMCID: PMC7642142.

[34] Hintze BJ, Lewis SM, Richardson JS, Richardson DC. Molprobity's ultimate rotamer-library distributions for model validation. Proteins. 2016 Sep;84(9):1177-89. doi: 10.1002/prot.25039. Epub 2016 Jun 23. PMID: 27018641; PMCID: PMC4983197.

[35] Cui, X., Li, S.C., Bu, D. et al. Protein Structure Idealization: How accurately is it possible to model protein structures with dihedral angles?. Algorithms Mol Biol 8, 5 (2013). https://doi.org/10.1186/1748-7188-8-5

[36] Taler-Verčič A, Hasanbašić S, Berbić S, Stoka V, Turk D, Žerovnik E. Proline Residues as Switches in Conformational Changes Leading to Amyloid Fibril Formation. Int J Mol Sci. 2017 Mar 7;18(3):549. doi: 10.3390/ijms18030549. PMID: 28272335; PMCID: PMC5372565.

[37] Schwede T, Kopp J, Guex N, Peitsch MC. SWISS-MODEL: An automated protein homology-modelling server. Nucleic Acids Res. 2003 Jul 1;31(13):3381-5. doi: 10.1093/nar/gkg520. PMID: 12824332; PMCID: PMC168927.

[38] Zheng W, Zhang C, Bell EW, Zhang Y. I-TASSER gateway: A protein structure and function prediction server powered by XSEDE. Future Gener Comput Syst. 2019 Oct;99:73-85. doi: 10.1016/j.future.2019.04.011. Epub 2019 Apr 9. PMID: 31427836; PMCID: PMC6699767.

[39] Xu J, Zhang Y. How significant is a protein structure similarity with TM-score = 0.5? Bioinformatics. 2010 Apr 1;26(7):889-95. doi: 10.1093/bioinformatics/btq066. Epub 2010 Feb 17. PMID: 20164152; PMCID: PMC2913670.

[40] Roy A, Kucukural A, Zhang Y. I-TASSER: a unified platform for automated protein structure and function prediction. Nat Protoc. 2010 Apr;5(4):725-38. doi: 10.1038/nprot.2010.5. Epub 2010 Mar 25. PMID: 20360767; PMCID: PMC2849174.

[41] Kufareva I, Abagyan R. Methods of protein structure comparison. Methods Mol Biol. 2012;857:231-57. doi: 10.1007/978-1-61779-588-6_10. PMID: 22323224; PMCID: PMC4321859.

[42] Deng H, Jia Y, Zhang Y. 3DRobot: automated generation of diverse and well-packed protein structure decoys. Bioinformatics. 2016 Feb 1;32(3):378-87. doi: 10.1093/bioinformatics/btv601. Epub 2015 Oct 14. PMID: 26471454; PMCID: PMC5006309.

[43] Zhang Y. I-TASSER: fully automated protein structure prediction in CASP8. Proteins. 2009;77 Suppl 9(Suppl 9):100-13. doi: 10.1002/prot.22588. PMID: 19768687; PMCID: PMC2782770.

[44] Cormier KW, Larsen B, Gingras AC, Woodgett JR. Interactomes of Glycogen Synthase Kinase-3 Isoforms. J Proteome Res. 2023 Mar 3;22(3):977-989. doi: 10.1021/acs.jproteome.2c00825. Epub 2023 Feb 13. PMID: 36779422; PMCID: PMC9990120.

[45] Itoh K, Antipova A, Ratcliffe MJ, Sokol S. Interaction of dishevelled and Xenopus axin-related protein is required for wnt signal transduction. Mol Cell Biol. 2000 Mar;20(6):2228-38. doi: 10.1128/MCB.20.6.2228-2238.2000. PMID: 10688669; PMCID: PMC110839.

[46] MacAulay K, Woodgett JR. Targeting glycogen synthase kinase-3 (GSK-3) in the treatment of Type 2 diabetes. Expert Opin Ther Targets. 2008 Oct;12(10):1265-74. doi: 10.1517/14728222.12.10.1265. PMID: 18781825; PMCID: PMC4485462.

[47] Hevey D. Network analysis: a brief overview and tutorial. Health Psychol Behav Med. 2018 Sep

25;6(1):301-328. doi: 10.1080/21642850.2018.1521283. PMID: 34040834; PMCID: PMC8114409.

[48] González-Faune P, Sánchez-Arévalo I, Sarkar S, Majhi K, Bandopadhyay R, Cabrera-Barjas G, Gómez A, Banerjee A. Computational Study on Temperature Driven Structure-Function Relationship of Polysaccharide Producing Bacterial Glycosyl Transferase Enzyme. Polymers (Basel). 2021 May 28;13(11):1771. doi: 10.3390/polym13111771. PMID: 34071348; PMCID: PMC8198650.

[49] He K, Gan WJ. Wnt/β-Catenin Signaling Pathway in the Development and Progression of Colorectal Cancer. Cancer Manag Res. 2023 May 23;15:435-448. doi: 10.2147/CMAR.S411168. PMID: 37250384; PMCID: PMC10224676.

[50] Hoffmeister L, Diekmann M, Brand K, Huber R. GSK3: A Kinase Balancing Promotion and Resolution of Inflammation. Cells. 2020 Mar 28;9(4):820. doi: 10.3390/cells9040820. PMID: 32231133; PMCID: PMC7226814.

[51] Mirzoev TM, Sharlo KA, Shenkman BS. The Role of GSK-3β in the Regulation of Protein Turnover, Myosin Phenotype, and Oxidative Capacity in Skeletal Muscle under Disuse Conditions. Int J Mol Sci. 2021 May 11;22(10):5081. doi: 10.3390/ijms22105081. PMID: 34064895; PMCID: PMC8151958.

[52] Sahin I, Eturi A, De Souza A, Pamarthy S, Tavora F, Giles FJ, Carneiro BA. Glycogen synthase kinase-3 beta inhibitors as novel cancer treatments and modulators of antitumor immune responses. Cancer Biol Ther. 2019;20(8):1047-1056. doi: 10.1080/15384047.2019.1595283. Epub 2019 Apr 12. PMID: 30975030; PMCID: PMC6606036.

[53] McCubrey, J., Steelman, L., Bertrand, F. et al. Multifaceted roles of GSK-3 and Wnt/β-catenin in hematopoiesis and leukemogenesis: opportunities for therapeutic intervention. Leukemia **28**, 15–33 (2014). https://doi.org/10.1038/leu.2013.184.

[54] Ding L, Billadeau DD. Glycogen synthase kinase-3β: a novel therapeutic target for pancreatic cancer. Expert Opin Ther Targets. 2020 May;24(5):417-426. doi: 10.1080/14728222.2020.1743681. Epub 2020 Mar 21. PMID: 32178549; PMCID: PMC7539227.